Journal of Engineering Mathematics, Vol. 5, No. 2, April 1971
Wolters-Noordhoff Publishing–Groningen
Printed in the Netherlands

On Finite-Difference Methods for the Korteweg–de Vries Equation

A. C. VLIEGENTHART

Department of Mathematics, Delft University of Technology, The Netherlands

(Received October 1, 1970)

SUMMARY

The purpose of this paper is to set up and analyse difference schemes for solving the initial-value problem for the so-called Korteweg–de Vries equation. After the discussion of a difference scheme which is correctly centered in both space and time, the construction of difference schemes which implicitly contain the effect of dissipation is described.

1. Introduction

In the well-known publication by Korteweg and de Vries [1] on long waves in hydrodynamics, the so-called Korteweg–de Vries (KdV) equation was derived, which describes one-dimensional, shallow-water waves with small but finite amplitudes.

More recently, the KdV equation has been found to describe wave phenomena in plasma physics [2, 3], anharmonic crystals [4, 5] and bubble-liquid mixtures [6, 7]. The KdV equation is also relevant to the discussion of the interaction between nonlinearity and dispersion, just as the well-known Burgers equation shows the features of the interaction between nonlinearity and dissipation.

For appropriate initial functions Sjöberg and Lax [8, 9] have shown the existence and uniqueness of solutions of the KdV equation. Approximate solutions in the form of expansions were given by Broer [10], whilst Hoogstraten [11] obtained asymptotic solutions for slowly varying wavetrains.

Lax, Gardner *et al.* [9, 12] described analytic considerations concerning the existence of solitary waves in solutions of certain initial-value problems. Zabusky and Kruskal [13] encountered this appearance of solitary waves in studying the results of a numerical analysis.

In this paper we discuss three explicit finite-difference schemes for solving the initial-value problem for the KdV equation. The first scheme is correctly centered in both space and time and does not exhibit numerical damping. It has some features similar to the well-known leap-frog method, which is frequently employed in meteorological calculations. The second and third schemes may be used to construct solutions of discontinuous initial-value problems. The KdV approximation by itself does not take into account mechanisms of dissipation; however, we shall show how to set up these dissipative difference schemes, which have the effect of eliminating high wave number components. Here we have made use of the device for the construction of the Lax and Lax–Wendroff schemes [14, 15]. All schemes are conditionally stable. Dispersion at high wave numbers is a serious shortcoming which is, however, common to all difference approximations, as has become increasingly evident.

2. General Remarks

The KdV equation for long waves in shallow water may be written

$$\eta_t + \sqrt{gh_0}\,[1+\tfrac{3}{2}(\eta/h_0)]\,\eta_x + \tfrac{1}{6}\sqrt{gh_0}\,h_0^2\,\eta_{xxx} = 0\ ; \tag{2.1}$$

x denotes the coordinate along the horizontal bottom, t the time, $\eta(x, t)$ the local wave-height above the undisturbed depth h_0, and g the acceleration of gravity.

The subscripts in (2.1) indicate partial differentiation. Equation (2.1) is valid for comparable small values of a/h_0 and $(h_0/\lambda_0)^2$, where a and λ_0 denote the dominant amplitude and wave-length respectively. The non-dimensional parameters ε and μ will be used where

$$\varepsilon = a/h_0\,, \quad \mu = \tfrac{1}{6}(h_0/\lambda_0)^2\,,$$

and further we introduce the dimensionless variables

$$\bar{x} = x/\lambda_0\,, \quad \bar{t} = t\,\sqrt{gh_0}/\lambda_0\,, \quad \bar{\eta} = \tfrac{3}{2}\eta/(\varepsilon h_0)\,.$$

Having omitted the bars, substitution of these new variables into the equation (2.1) yields the equation

$$\eta_t + \eta_x + \varepsilon\eta\eta_x + \mu\eta_{xxx} = 0\,. \tag{2.2}$$

In the case of the dimensionless variables the speed of long, low waves, i.e. $\sqrt{gh_0}$, is unity, whilst the wave-height, the wave-length, as well as all derivatives of η to x and t are of order of magnitude one. For an arbitrary function $f(x)$ with f smooth enough whilst tending to zero sufficiently rapidly as $x \to \pm\infty$, Sjöberg [8] has shown that the KdV equation has a solution $\eta(x, t)$, with $\eta(x, 0) = f(x)$.

Lax [9] has shown that solutions of the KdV equation which together with all their x derivatives tend to zero as $x \to \pm\infty$, are uniquely determined by their initial values.

It is particularly interesting to note that the KdV equation is invariant to Galilean transformation: if $\eta(x, t)$ is a solution of (2.2), then the same is true for $\eta(x + \varepsilon\lambda t, t) - \lambda$, thus representing a one-parameter family of solutions.

By means of the new independent variable s, with $s = x - t$, equation (2.2) is transformed into the equation

$$\eta_t + \varepsilon\eta\eta_s + \mu\eta_{sss} = 0\,. \tag{2.3}$$

This form of the KdV equation will be used for the first part of our calculations.

3. Exact Solutions

We consider equation (2.3) in the case $\mu = 0$, i.e.

$$\eta_t + \varepsilon\eta\eta_s = 0\,. \tag{3.1}$$

Suppose that initially we have

$$\eta(s, 0) = f(s)\,, \tag{3.2}$$

where the function $f(s)$ is defined for all s in $(-\infty, \infty)$. It is well known that the equation $\eta_t g_s - \eta_s g_t = 0$ expresses the vanishing of the Jacobian $\partial(\eta, g)/\partial(s, t)$ with $g = g(s, t, \eta)$. The solution is given by

$$\eta(s, t) = W\{g[s, t, \eta(s, t)]\}\,,$$

and the solution of (3.1) is found to be

$$\eta(s, t) = f[s - \varepsilon t\eta(s, t)]\,. \tag{3.3}$$

The arbitrary function W has been determined by the initial condition (3.2).

From equation (3.3) we conclude that η is constant for unchanged values of $s - \varepsilon t\eta$, i.e. η is constant along the paths $s = \varepsilon\eta t +$ constant in the s, t-plane, which are the so-called characteristics.

The solution $\eta(s, t)$ remains bounded for increasing t, however, η steepens in the region of a negative slope and even becomes multi-valued. This is clear if one considers the relation $\eta_s = f'/(1 + \varepsilon t f')$, which is obtained by differentiation of (3.3) to s. If $f' < 0$, η_s becomes multi-valued at the time $t = -1/(\varepsilon f')$ and from this time on the characteristics intersect each other.

The characteristic which issues from the s-axis at $s = \zeta$ is given by $s - \zeta = \varepsilon f(\zeta)t$. Differentiating this equation to ζ gives $-1 = \varepsilon f'(\zeta)t$. Thus we have found the parameter representation of the envelope of the characteristics in the region of a negative slope for $t \geqq -1/(\varepsilon f')$:

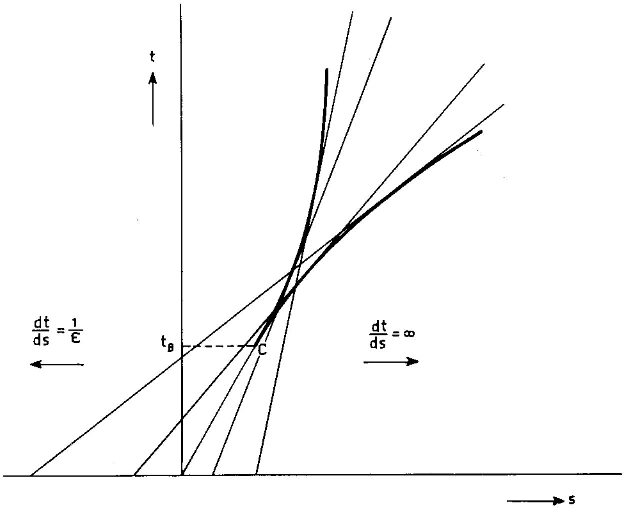

Figure 1. Characteristics and envelope with cusp C; $\eta(s,0)=\frac{1}{2}[1-\tanh(s/a)]$.

$$s=\zeta-f(\zeta)/f'(\zeta)$$
$$t=-1/[\varepsilon f'(\zeta)]\,. \tag{3.4}$$

Figure 1 shows the characteristics and the envelope with the cusp C in the case $f(s)=\frac{1}{2}[1-\tanh(s/a)]$, where a is some positive constant number. In this case formulas (3.4) give the equations

$$s=\zeta+a/[1+\tanh(\zeta/a)]$$
$$t=2(a/\varepsilon)\cosh^2(\zeta/a)\,,$$

for the envelope, and point C is given by $s=a$ and $t=2a/\varepsilon$. (3.5)

Results of numerical calculations also show the steepening of a negative slope in the case of non-vanishing dispersion. Before the solution becomes multi-valued, however, phenomena occur which are typical for the KdV equation (see next section).

If $\varepsilon=0$, equation (2.3) becomes $\eta_t+\mu\eta_{xxx}=0$. An exact solution in special cases can now be found by means of the Airy function of the first kind (see e.g. [10]). An example is given in the Appendix.

4. A Centered Finite-Difference Scheme

4.1. *Introduction*

Peregrine [16] introduced a difference scheme for the KdV equation which has first-order accuracy and yields some numerical damping. In this section we discuss another scheme which also has been used by Zabusky and Kruskal [13] and which is given by

$$\eta_j^{n+1}=\eta_j^{n-1}-\tfrac{1}{3}\varepsilon\frac{\Delta t}{\Delta s}(\eta_{j+1}^n+\eta_j^n+\eta_{j-1}^n)(\eta_{j+1}^n-\eta_{j-1}^n)-\mu\frac{\Delta t}{(\Delta s)^3}(\eta_{j+2}^n-2\eta_{j+1}^n+2\eta_{j-1}^n-\eta_{j-2}^n)\,, \tag{4.1}$$

where $\eta_j^n=\eta(j\Delta s, n\Delta t)$; j and n are integers. This scheme is consistent with equation (2.3) and the truncation error is $O[(\Delta t)^3]+O[\Delta t(\Delta s)^2]$.

For the initial step one may use the uncentered scheme

$$\eta_j^1=\eta_j^0-\tfrac{1}{6}\varepsilon\frac{\Delta t}{\Delta s}(\eta_{j+1}^0+\eta_j^0+\eta_{j-1}^0)(\eta_{j+1}^0-\eta_{j-1}^0)-\tfrac{1}{2}\mu\frac{\Delta t}{(\Delta s)^3}(\eta_{j+2}^0-2\eta_{j+1}^0+2\eta_{j-1}^0-\eta_{j-2}^0)\,. \tag{4.2}$$

4.2. *General considerations*

It is well known that at the early stages an instability develops in a very small region. Therefore, if the solution is slowly varying, an instability may be predicted by means of a stability analysis of the localized version of the difference scheme, that is, in the case of scheme (4.1), of the equation

$$\eta_j^{n+1} = \eta_j^{n-1} - \varepsilon\eta \frac{\Delta t}{\Delta s}(\eta_{j+1}^n - \eta_{j-1}^n) - \mu \frac{\Delta t}{(\Delta s)^3}(\eta_{j+2}^n - 2\eta_{j+1}^n + 2\eta_{j-1}^n - \eta_{j-2}^n), \tag{4.3}$$

where η in the coefficient of the second term on the right-hand side has some local value.

The Fourier series representation of the exact solution of equation (4.3) which satisfies prescribed initial data can be written

$$\eta_j^n = \sum_{-\infty}^{\infty}{}_{(k)}\, C_k [g(k)]^n \exp(ikj\Delta s). \tag{4.4}$$

To determine the so-called amplification factor $g(k)$ we substitute the kth term in place of η_j^n into (4.3) and, after some manipulation, we obtain

$$g^2 + 2i \sin\xi \frac{\Delta t}{\Delta s}\left[\varepsilon\eta - 2\frac{\mu}{(\Delta s)^2}(1-\cos\xi)\right] g - 1 = 0, \tag{4.5}$$

where $\xi = k\Delta s$.

The product of the roots of the quadratic equation equals -1. Therefore, for stability, it will be necessary that the modulus of both roots be equal to unity.

Let us put

$$\sin\theta = \sin\xi \frac{\Delta t}{\Delta s}\left[\varepsilon\eta - 2\frac{\mu}{(\Delta s)^2}(1-\cos\xi)\right]; \tag{4.6}$$

in the stable case we then have $g(k) = \pm\exp(\mp i\theta)$, and

$$\eta_j^n = \sum_{-\infty}^{\infty}{}_{(k)}\, C_k [\alpha_k \exp(-i\theta n) + \beta_k(-1)^n \exp(i\theta n)] \exp(ij\xi).$$

The coefficients α_k and β_k are determined by the solutions at $t=0$ and $t=\Delta t$, i.e. from the equations

$$\alpha_k + \beta_k = 1$$
$$\alpha_k \exp(-i\theta) - \beta_k \exp(i\theta) = 1 - i\sin\theta.$$

The last equation is obtained from the localized version of scheme (4.2). Thus, we arrive at the exact solution of the localized form of the difference schemes (4.1) and (4.2), which satisfies the prescribed initial data,

$$\eta_j^n = \sum_{-\infty}^{\infty}{}_{(k)}\, C_k [(1+\cos\theta)/(2\cos\theta)\exp(-i\theta n) - $$
$$- (1-\cos\theta)/(2\cos\theta)(-1)^n \exp(i\theta n)] \exp(ij\xi). \tag{4.7}$$

This solution may be compared with the corresponding Fourier series solution of equation (2.3) with constant coefficients,

$$\eta(s, t) = \sum_{-\infty}^{\infty}{}_{(k)}\, C_k \exp[i(ks - lt)]. \tag{4.8}$$

The wave number k and the frequency $l(k)$ are related by means of the so-called frequency relation

$$l(k) = \varepsilon\eta k - \mu k^3, \tag{4.9}$$

which is found by substitution of the kth term of (4.8) into the linearized equation (2.3). It may be noted that, if θ is replaced by $l\Delta t$, equation (4.6) approaches the frequency relation if Δt and Δs go to zero. The actual meaning of θ is obvious now.

The first wave solution of (4.7) approaches the solution (4.8) if Δt and Δs tend to zero. The phase speed of this wave is given by

$$\frac{\theta}{\xi\,\Delta t/\Delta s}=\frac{1}{\xi\,\Delta t/\Delta s}\arcsin\left\{\sin\xi\,\frac{\Delta t}{\Delta s}\left[\varepsilon\eta-2\,\frac{\mu}{(\Delta s)^2}\,(1-\cos\xi)\right]\right\},$$

whilst the phase speed of the corresponding wave component $C_k \exp[i(ks-lt)]$ is l/k. For the ratio $Q(k)$ of these two velocities we may derive

$$Q(k)=\arcsin\left\{\sin\xi\,\frac{\Delta t}{\Delta s}\left[\varepsilon\eta-2\,\frac{\mu}{(\Delta s)^2}\,(1-\cos\xi)\right]\right\}\Big/\left(\xi\,\frac{\Delta t}{\Delta s}\left[\varepsilon\eta-\frac{\mu}{(\Delta s)^2}\,\xi^2\right]\right). \tag{4.10}$$

During the time which passes from $t=0$ to $t=2\pi/l$ the component $C_k \exp[i(ks-lt)]$ propagates over its wave-length, and the phase shift caused by the discretization and which corresponds to the velocity ratio $Q(k)$ is then given by $2\pi[1-Q(k)]$.

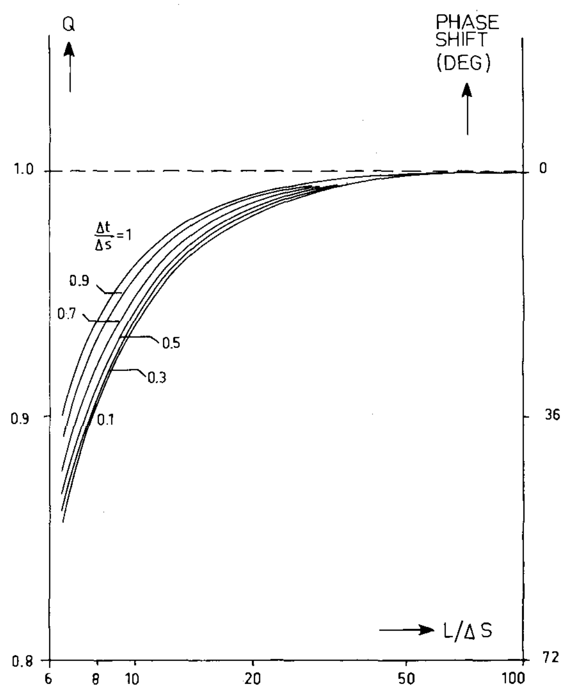

Figure 2. Scheme (4.1): Velocity ratio and phase shift; $\varepsilon\eta=0.7$, $\mu/(\Delta s)^2=0.1$.

Figure 2 shows a set of curves for Q as given by formula (4.10), together with the corresponding phase shift, versus $L/\Delta s$. L is the wave-length, i.e., $L/\Delta s=2\pi/\xi$.

The second wave solution of (4.7) is of the type of a so-called computational wave (see [17]) and exists because of the second order form of scheme (4.1). This wave propagates into the wrong direction, the sign of the amplitude changes at every time-step and the amplitude tends to zero if $\Delta t\to 0$. The last quality makes it possible to suppress the computational wave in actual calculations.

From equation (4.7) we conclude that no numerical damping (see [18]) is present. However, as we show next, wave amplitudes may possibly increase indefinitely with n. We have assumed so far that the modulus of the right-hand member of equation (4.6) is not greater than unity. If this is not true, it can easily be shown that the roots of equation (4.5) are

$$g(k)=\exp\left[-\tfrac{1}{2}\pi i+\cosh^{-1}(\ \sin\theta)\right]\quad\text{if}\quad \sin\theta>\ 1\,,$$

and

$$g(k)=\exp\left[\ \tfrac{1}{2}\pi i+\cosh^{-1}(-\sin\theta)\right]\quad\text{if}\quad \sin\theta<-1\,.$$

In both cases we find two solutions for g satisfying (4.5) and one of these solutions will in both cases increase indefinitely with n. It will be clear that for stability we require

$$\left|\sin\xi\,\frac{\Delta t}{\Delta s}\left[\varepsilon\eta-2\frac{\mu}{(\Delta s)^2}(1-\cos\xi)\right]\right|\leqq 1\,,$$

and this yields the stability condition

$$\frac{\Delta t}{\Delta s}\left[\varepsilon|\eta|+4\frac{\mu}{(\Delta s)^2}\right]\leqq 1\,. \tag{4.11}$$

If η is periodic in s, or if η and the s derivatives of η disappear at the finite of infinite ends of some interval, constants of motion exist. Among these the two most simple are

$$\int \eta\, ds\,, \tag{4.12}$$

and

$$\int \tfrac{1}{2}\eta^2\, ds\,, \tag{4.13}$$

which are obtained by integration of the equations $\eta_t+(\frac{1}{2}\varepsilon\eta^2+\mu\eta_{ss})_s=0$, and $(\frac{1}{2}\eta^2)_t+(\frac{1}{3}\varepsilon\eta^3+\mu\eta\eta_{ss}-\frac{1}{2}\mu\eta_s^2)_s=0$, in that order. The last equation is found after multiplication of (2.3) by η.

Summation of (4.1) over all net points of the interval $0\leqq s\leqq J\Delta s$ yields

$$\sum_{(j)\,0}^{J}(\eta_j^{n+1}-\eta_j^{n-1})=-\tfrac{1}{3}\varepsilon\frac{\Delta t}{\Delta s}\left[-(\eta_{-1})^2-\eta_{-1}\eta_0-(\eta_0^2)+(\eta_J^2)+\eta_J\eta_{J+1}+(\eta_{J+1})^2\right]$$

$$-\mu\frac{\Delta t}{(\Delta s)^3}\left[-\eta_{-2}+\eta_{-1}+\eta_0-\eta_1+\eta_{J-1}-\eta_J-\eta_{J+1}+\eta_{J+2}\right],$$

where all values in the right-hand member have been taken at the time $t=n\Delta t$. The right-hand side of this equation will disappear if η equals zero at the left hand and right boundaries. The same is true if η is periodic, which may be expressed by the boundary conditions

$$\eta_{-2}=\eta_{J-1}\qquad \eta_{J+1}=\eta_0$$
$$\eta_{-1}=\eta_J\qquad \eta_{J+2}=\eta_1\,.$$

Obviously, (4.12) though in discrete form, is a constant of motion in the case of appropriate boundary conditions. In [13] a decisive answer is given concerning (4.13); in this case the terms

$$\tfrac{1}{6}(\Delta t)^2\sum_{(j)\,0}^{J}\eta_j(\eta_j)_{ttt}+O[(\Delta t)^4]$$

should be neglected. The conclusion is that scheme (4.1) is momentum- and energy-conserving.

4.3. *Numerical Results*

By using a solitary wave as given by (4.14) with $\eta_0=1$ and $\eta_\infty=0$ as initial function, it became clear to us that condition (4.11) is too stringent: in the case of $\varepsilon=\mu=0.1$ the process even remained stable for $\Delta s=0.2$, $\Delta t=0.03$, though (4.11) was exceeded by about 50%. The process however was unstable at the early stages when we had chosen $\Delta t=0.04$, whilst leaving the other values unchanged.

Figure 3 shows the results of the schemes (4.1) and (4.2) with initially

$$\eta(s,0)=\tfrac{1}{2}[1-\tanh(s-25)/5]\,.$$

Physically these results represent among others the development of an undular bore in shallow water and a collisionless shock in plasmas.

From (3.5) we conclude that in the case $\mu=0$ the solution of this problem would become multi-valued at the time $t=50$. By varying the values of the parameters ε and μ, it appeared that with increasing ε as well as with decreasing μ the pulses became narrower.

The appearance of solitary waves in certain solutions of the KdV equation has been discussed by Zabusky and Kruskal [13]. The upper parts of the pulses in Figure 3 also satisfy the equation of a solitary wave, i.e. the steady state solution of equation (2.3) which goes to some constant

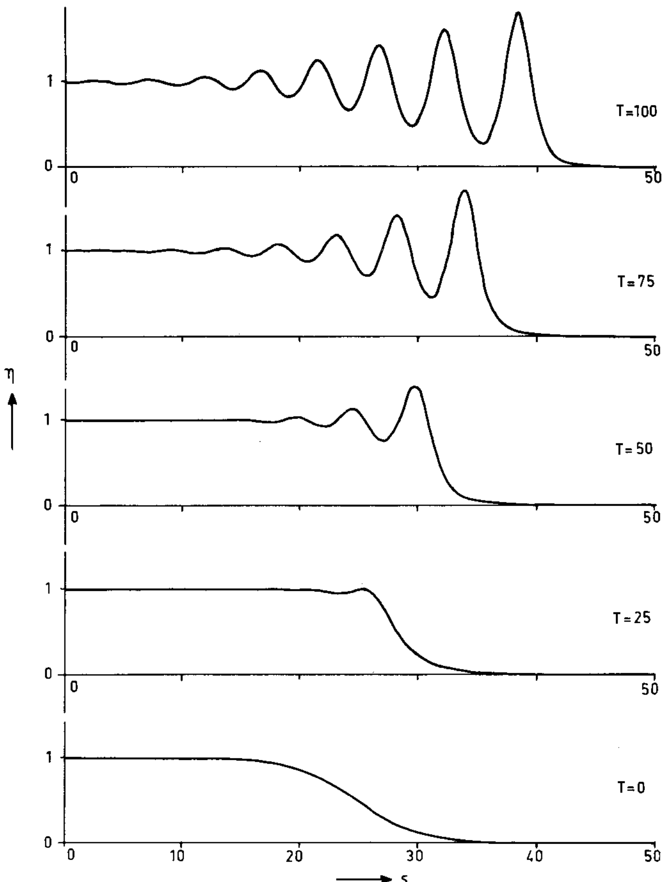

Figure 3. Initial-value problem with $\eta(s, 0) \equiv \frac{1}{2}\left[1 - \tanh\left(\frac{s-25}{5}\right)\right]$; $\varepsilon = 0.2$, $\mu = 0.1$, $\Delta s = 0.4$, $\Delta t = 0.05$.

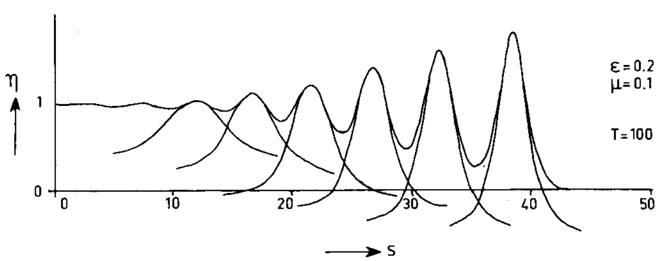

Figure 4. Same solution at $t = 100$ with corresponding solitary waves.

value η_∞ as s tends to $\pm\infty$. After substitution of $\eta(s, t) = N(s - ct)$ into equation (2.3) and integrating twice, the steady state solution is found to be

$$\eta = \eta_\infty + (\eta_0 - \eta_\infty) \operatorname{sech}^2 (s - s_0) \sqrt{\tfrac{1}{12}(\varepsilon/\mu)(\eta_0 - \eta_\infty)}\,, \tag{4.14}$$

with

$$c = \varepsilon\eta_\infty + \tfrac{1}{3}\varepsilon(\eta_0 - \eta_\infty)\ ; \tag{4.15}$$

η_0 denotes the value of η at $s = s_0$.

From equation (4.14) we derive

$$\eta_\infty = \eta_0 - \sqrt{6(\mu/\varepsilon)\,|\eta_{ss}|_{s=s_0}}\,, \tag{4.16}$$

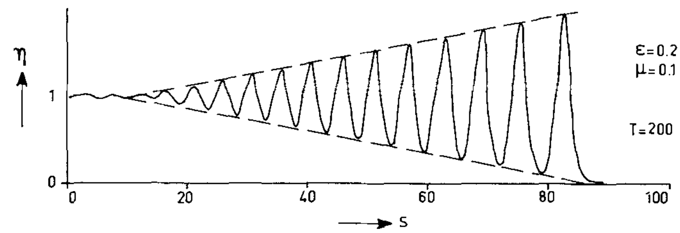

Figure 5. Same solution at $t=200$ showing the linear variation of the amplitudes.

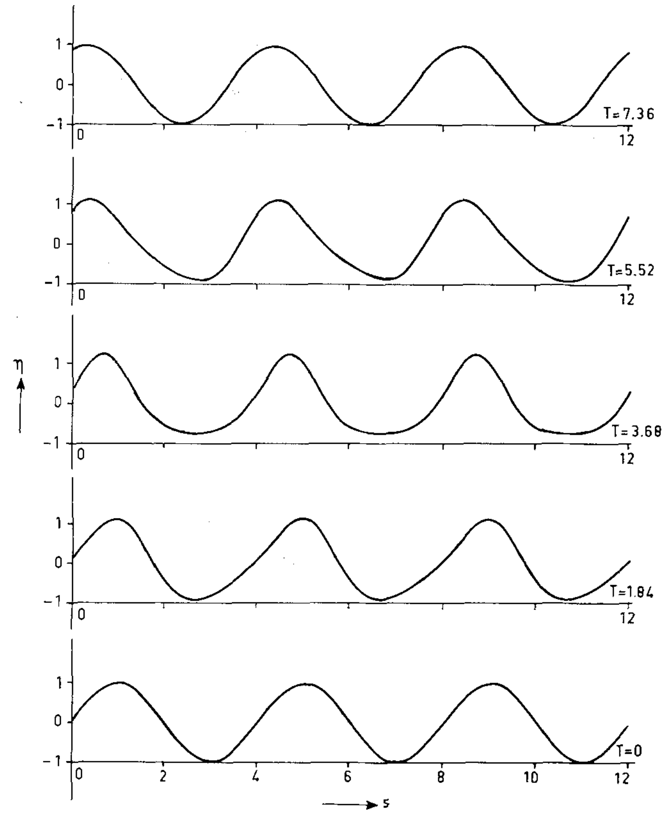

Figure 6. Initial-value problem with $\eta(s, 0) \equiv \sin\frac{1}{2}\pi s$; $\varepsilon=0.1$, $\mu=0.04$, $\Delta s=0.2$, $\Delta t=0.04$.

by differentiating twice.

From the results at $t=100$ (see Fig. 3) we noted the values of s_0, η_0, and, after numerical differentiation, of η_{ss} at $s=s_0$. Formula (4.16) yields the corresponding values of η_∞.

Figure 4 shows the pulses at $t=100$ again together with graphs of relation (4.14) after substitution of the observed values of s_0, η_0 and η_∞. Especially the upper part of the pulse on the extreme right which is the most stationary appears to be approximated well by the solitary wave solution. The values of c as given by formula (4.15) after substitution of the values of η_0 and η_∞ obtained as described above, are smaller than the observed velocities of the waves.

In Figure 5 is shown the solution of the same problem at $t=200$. It appears that the amplitudes of the waves vary approximately linearly.

Another interesting problem is shown in Figure 6 where a sinusoidal wave form is given as initial function, $\eta(s, 0)=\sin\frac{1}{2}\pi s$. Apart from a phase shift, the initial solution is approximately present again at the time $t=7.36$. The time at which the negative slopes of the solution would become multi-valued if $\mu=0$ is in this case $t=6.37$. From our numerical results we conclude that the recurrence time is almost independent of ε and proportional to $1/\mu$. In the case $\varepsilon=0$

the recurrence time drops to zero, as the solution is then given by $\eta(s, t) = \sin(\frac{1}{2}\pi s + \frac{1}{8}\pi^3 \mu t)$. The recurrence time depends strongly on the wave-length, as it appeared that the recurrence time decreased quickly when the wave-length was diminished.

In [13] the recurrence of the sinusoidal wave form is described for $\varepsilon = 1$ and $\mu = 4.84 \times 10^{-4}$. In this case of dominating nonlinearity solitary waves also appear.

5. Dissipative Difference Schemes

5.1. *Introduction*

The difference scheme (4.1) for solving numerically the initial-value problem for the partial differential equation (2.3) is correctly centered in both space and time. Consequently, in the stable case we have found for the amplification factor $g(k)$ of the kth wave component that $|g(k)| = 1$ is valid for all values of k which must be considered. The exact amplification factor of equation (2.3) is given by $\exp(-il\Delta t)$, where the frequency $l(k)$ is determined by the frequency relation (4.9). Since a real value of $l(k)$ corresponds with each real value of k, the modulus of the exact amplification factor also equals unity. Therefore, within the scope of convergence, one may set up the property $|g(k)| = 1$ for a difference approximation to (2.3).

In some cases, however, difference schemes may be needed which eliminate unwanted short-wavelength components as the calculation progresses. Such difference schemes, which are generally called dissipative, are not centered correctly in both space and time (see e.g. [19]), but they are given the property $|g(k)| < 1$ by, for instance, one-sided time differences. In this connection it should be pointed out that here we have to deal with a mild strengthening of the stability condition: Suppose that the calculations are carried from $t = 0$ to $t = T$. For (Lax–Richtmyer) stability is then required that for some positive τ,

$$[g(k)]^n \quad \text{for} \quad \begin{cases} 0 < \Delta t < \tau \\ 0 \leqq n\Delta t \leqq T \\ \text{all } k \text{ in consideration} \end{cases}$$

are uniformly bounded. This yields (see [20]) the necessary and sufficient stability condition $|g(k)| \leqq 1 + O(\Delta t)$.

5.2. *Scheme Accurate to the First Order*

We start from the Taylor expansion

$$\eta_j^{n+1} = \eta_j^n + \Delta t \eta_t |_j^n + O[(\Delta t)^2] , \tag{5.1}$$

where $\eta(s, t) = \eta(j\Delta s, n\Delta t)$ is denoted by n_j^n.

Evaluating the second term of this expansion by means of equation (2.3) yields

$$\eta_j^{n+1} = \eta_j^n - \Delta t(\varepsilon\eta\eta_s + \mu\eta_{sss}) |_j^n + O[(\Delta t)^2] .$$

The s-derivatives are replaced by symmetric difference quotients, giving the explicit difference scheme

$$\eta_j^{n+1} = \eta_j^n - \tfrac{1}{4}\varepsilon \frac{\Delta t}{\Delta s} [(\eta_{j+1}^n)^2 - (\eta_{j-1}^n)^2] - \tfrac{1}{2}\mu \frac{\Delta t}{(\Delta s)^3} (\eta_{j+2}^n - 2\eta_{j+1}^n + 2\eta_{j-1}^n - \eta_{j-2}^n) . \tag{5.2}$$

We linearize equation (5.2) and obtain an equation with constant coefficients:

$$\eta_j^{n+1} = \eta_j^n - \tfrac{1}{2}\varepsilon\eta \frac{\Delta t}{\Delta s} (\eta_{j+1}^n - \eta_{j-1}^n) - \tfrac{1}{2}\mu \frac{\Delta t}{(\Delta s)^3} (\eta_{j+2}^n - 2\eta_{j+1}^n + 2\eta_{j-1}^n - \eta_{j-2}^n) .$$

The kth term of series (4.4) is substituted into this equation which finally gives for the corresponding local amplification factor $g(k)$ the formula

$$g(k)=1-i\sin\xi\,\frac{\Delta t}{\Delta s}\left[\varepsilon\eta-2\frac{\mu}{(\Delta s)^2}(1-\cos\xi)\right],$$

with $\xi=k\Delta s$ as before.

From the last equation we conclude that scheme (5.2) is unconditionally unstable.

Consider, however, the modified form of (5.2),

$$\eta_j^{n+1}=\tfrac{1}{2}(\eta_{j+1}^n+\eta_{j-1}^n)-\tfrac{1}{4}\varepsilon\frac{\Delta t}{\Delta s}\left[(\eta_{j+1}^n)^2-(\eta_{j-1}^n)^2\right]-\tfrac{1}{2}\mu\frac{\Delta t}{(\Delta s)^3}(\eta_{j+2}^n-2\eta_{j+1}^n+2\eta_{j-1}^n-\eta_{j-2}^n)\,. \quad (5.3)$$

This scheme has first-order accuracy, the truncation error being $O[(\Delta t)^2]+O[(\Delta s)^2]$. After linearizing, the local amplification factor of scheme (5.3) is given by

$$g(k)=\cos\xi-i\sin\xi\,\frac{\Delta t}{\Delta s}\left[\varepsilon\eta-2\frac{\mu}{(\Delta s)^2}(1-\cos\xi)\right].$$

Let us put

$$\beta=\frac{\Delta t}{\Delta s}\left[\varepsilon\eta-2\frac{\mu}{(\Delta s)^2}(1-\cos\xi)\right].$$

Then we have

$$g(k)=\cos\xi-i\beta\sin\xi\,, \quad (5.4)$$

and

$$|g(k)|^2=1-(1-\beta^2)\sin^2\xi\,.$$

For stability $|\beta|\leqq 1$ is required. For actual damping of the wave components, i.e. to fulfil $|g(k)|<1$, we have to require $|\beta|<1$, which then gives the condition

$$\frac{\Delta t}{\Delta s}\left[\varepsilon|\eta|+4\frac{\mu}{(\Delta s)^2}\right]<1\,. \quad (5.5)$$

This condition being satisfied, the amplitude damping behaves like ξ^2. To obtain more insight about the amplitude and phase error caused by the discretization, we recall the complex propagation factor $T(k)$ as introduced by Leendertse [21],

$$T(k)=\exp[i(ks-l't)]/\exp[i(ks-lt)]\;;$$

l' denotes the frequency in the case of the difference approximation and is to be determined from

$$g(k)=\exp(-il'\Delta t)\,. \quad (5.6)$$

After the time $t=2\pi/l$, the wave component with frequency l has propagated over its wavelength once and we have

$$|T(k)|=\exp[2\pi\,\mathrm{Im}\,(l')/l]\,, \quad (5.7)$$

and

$$\arg[T(k)]=2\pi[1-\mathrm{Re}(l')/l]\,. \quad (5.8)$$

For the kth component $|T|$ and $\arg(T)$ will, in the same order, represent measures of the amplitude and phase error. In addition, we define the velocity ratio $Q(k)$ by the relationship $Q(k)=\mathrm{Re}(l')/l$, so that we have

$$\arg[T(k)]=2\pi[1-Q(k)]\,. \quad (5.9)$$

Using equations (4.9), (5.4) and (5.6) we obtain for scheme (5.3):

$$|T(k)|=(\cos^2\xi+\beta^2\sin^2\xi)^{\pi\Big/\left(\xi\frac{\Delta t}{\Delta s}\left[\varepsilon\eta-\frac{\mu}{(\Delta s)^2}\xi^2\right]\right)} \quad (5.10)$$

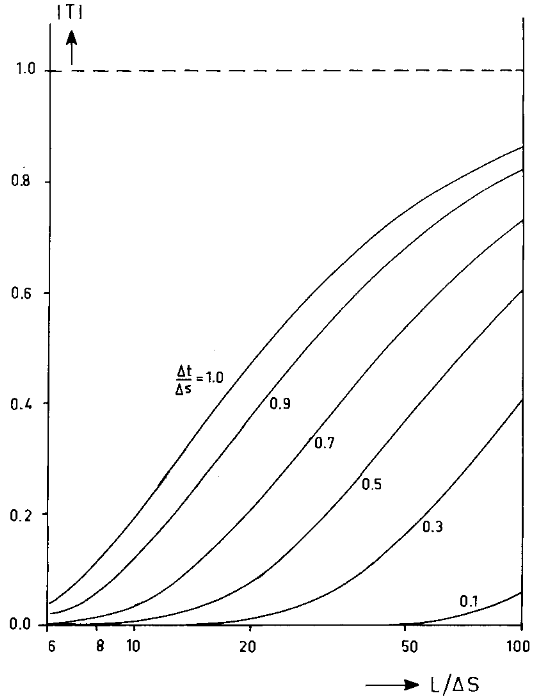

Figure 7. Scheme (5.3): Numerical damping as given by (5.10); $\varepsilon\eta = 0.7$, $\mu/(\Delta s)^2 = 0.1$.

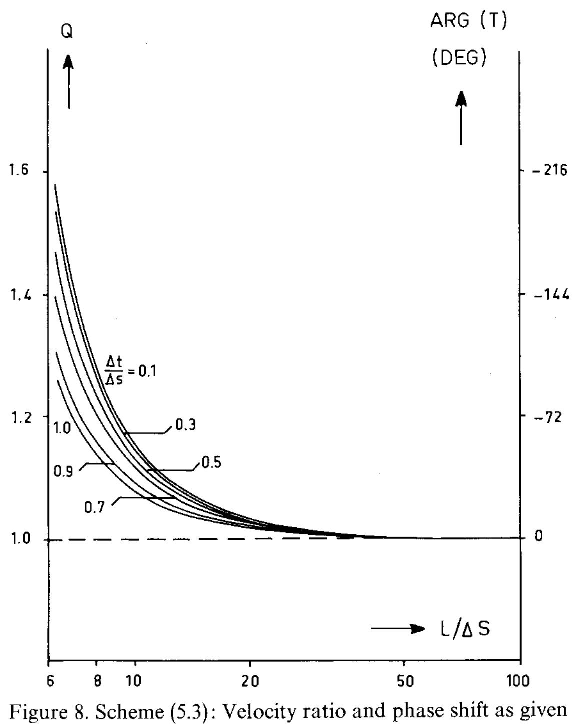

Figure 8. Scheme (5.3): Velocity ratio and phase shift as given by (5.11) and (5.9); $\varepsilon\eta = 0.7$, $\mu/(\Delta s)^2 = 0.1$.

and $$Q(k) = \arctan(\beta \tan \xi) \Big/ \left(\xi \frac{\Delta t}{\Delta s} \left[\varepsilon\eta - \frac{\mu}{(\Delta s)^2} \xi^2 \right] \right) . \tag{5.11}$$

Figures 7 and 8 are graphs of the equations (5.9) through (5.11); L denotes the wave-length again. We may note that the short wave components are especially affected. Both damping and dispersion occur. For $\xi \ll 1$, $\sin \xi \simeq \xi$ and $\cos \xi \simeq 1 - \frac{1}{2}\xi^2$ are valid. Then,

$$g(k) = 1 - i\xi \frac{\Delta t}{\Delta s}\left[\varepsilon\eta - \frac{\mu}{(\Delta s)^2}\xi^2\right] + O(\xi^2),$$

and, modulo terms of second order in ξ,

$$g(k) = \exp\left\{-i\xi \frac{\Delta t}{\Delta s}\left[\varepsilon\eta - \frac{\mu}{(\Delta s)^2}\xi^2\right]\right\}.$$

This is the exact amplification factor of equation (2.3), i.e. $\exp(-il\Delta t)$, with $l(k)$ as given by (4.9). We conclude that the amplification factor just like the difference operator is approximated with first-order accuracy, as required by the theory (see [20]).

If $\mu = 0$, scheme (5.3) reduces to the Lax scheme [14] as applied to the equation $\eta_t + \varepsilon\eta\eta_s = 0$.

5.3. *Scheme Accurate to the Second Order*

In this section we shall construct a dissipative difference scheme accurate to the second order for the KdV equation in the form

$$\eta_t + \eta_x + \varepsilon\eta\eta_x + \mu\eta_{xxx} = 0 \tag{5.12}$$

(see Chapter 2).

Substitution of the Fourier term $\exp[i(kx - lt)]$ into the localized form of equation (5.12) gives the appropriate frequency relation

$$l(k) = k(1 + \varepsilon\eta) - \mu k^3 . \tag{5.13}$$

We extend the Taylor expansion (5.1) by one term to become

$$\eta_j^{n+1} = \eta_j^n + \Delta t \eta_t|_j^n + \tfrac{1}{2}(\Delta t)^2 \eta_{tt}|_j^n + O[(\Delta t)^3] . \tag{5.14}$$

By introducing dimensionless variables as described in Chapter 2, η and the derivatives of η with respect to x and t are all of order of magnitude one. Furthermore, the equation (5.12) by itself is an approximation such that the squares and products of the parameters ε and μ are vanishingly small (see also [22]).

The t-derivatives in the expansion (5.14) are replaced by x-derivatives by virtue of

$$\eta_t = -\eta_x - \varepsilon\eta\eta_x - \mu\eta_{xxx}, \quad \text{and} \quad \eta_{tt} = \eta_{xx} + 2\varepsilon(\eta\eta_x)_x + 2\mu\eta_{xxxx} .$$

The second relation is obtained by differentiating the first with respect to t and replacing the t-derivatives by x-derivatives, neglecting the terms with squares and products of ε and μ. Substitution of these two relations into (5.14) yields

$$\eta_j^{n+1} = \eta_j^n - \Delta t[(1 + \varepsilon\eta)\eta_x + \mu\eta_{xxx}]|_j^n + (\Delta t)^2[\tfrac{1}{2}\eta_{xx} + \varepsilon(\eta\eta_x)_x + \mu\eta_{xxxx}]|_j^n + O[(\Delta t)^3] . \tag{5.15}$$

We replace the x-derivatives in (5.15) by symmetric difference quotients to obtain the scheme

$$\begin{aligned}
\eta_j^{n+1} = \eta_j^n &- \tfrac{1}{2}\frac{\Delta t}{\Delta x}[\eta_{j+1}^n(1 + \tfrac{1}{2}\varepsilon\eta_{j+1}^n) - \eta_{j-1}^n(1 + \tfrac{1}{2}\varepsilon\eta_{j-1}^n)] \\
&- \tfrac{1}{2}\mu \frac{\Delta t}{(\Delta x)^3}(\eta_{j+2}^n - 2\eta_{j+1}^n + 2\eta_{j-1}^n - \eta_{j-2}^n) \\
&+ \tfrac{1}{2}\left(\frac{\Delta t}{\Delta x}\right)^2(\eta_{j+1}^n - 2\eta_j^n + \eta_{j-1}^n) \\
&+ \tfrac{1}{2}\varepsilon\left(\frac{\Delta t}{\Delta x}\right)^2[(\eta_{j+1}^n + \eta_j^n)(\eta_{j+1}^n - \eta_j^n) - (\eta_j^n + \eta_{j-1}^n)(\eta_j^n - \eta_{j-1}^n)] \\
&+ \mu\frac{(\Delta t)^2}{(\Delta x)^4}(\eta_{j+2}^n - 4\eta_{j+1}^n + 6\eta_j^n - 4\eta_{j-1}^n + \eta_{j-2}^n) .
\end{aligned}$$

This scheme is accurate to the second order, as the truncation error is $O[(\Delta t)^3]+O[\Delta t(\Delta x)^2]$. However, computer tests using small values of the mesh-sizes, show clearly that the scheme is unconditionally unstable. We obtained stability here after the addition to the expansion (5.15) of the terms

$$(\Delta t)^2\,[\varepsilon\mu\eta\eta_{xxxx}+\tfrac{1}{2}\mu^2\eta_{xxxxxx}]|_j^n$$

which are, in fact, negligibly small.

Replacing, as before, the x-derivatives by symmetric difference quotients, we finally obtain the scheme

$$\begin{aligned}[\eta_{j+1}^{n} = \eta_j^n &-\tfrac{1}{2}\frac{\Delta t}{\Delta x}\,[\eta_{j+1}^n(1+\tfrac{1}{2}\varepsilon\eta_{j+1}^n)-\eta_{j-1}^n(1+\tfrac{1}{2}\varepsilon\eta_{j-1}^n)]\\
&-\tfrac{1}{2}\mu\frac{\Delta t}{(\Delta x)^3}\,(\eta_{j+2}^n-2\eta_{j+1}^n+2\eta_{j-1}^n-\eta_{j-2}^n)\\
&+\tfrac{1}{2}\left(\frac{\Delta t}{\Delta x}\right)^2(\eta_{j+1}^n-2\eta_j^n+\eta_{j-1}^n)\\
&+\tfrac{1}{2}\varepsilon\left(\frac{\Delta t}{\Delta x}\right)^2[(\eta_{j+1}^n+\eta_j^n)(\eta_{j+1}^n-\eta_j^n)-(\eta_j^n+\eta_{j-1}^n)(\eta_j^n-\eta_{j-1}^n)]\\
&+\mu\frac{(\Delta t)^2}{(\Delta x)^4}(1+\varepsilon\eta_j^n)(\eta_{j+2}^n-4\eta_{j+1}^n+6\eta_j^n-4\eta_{j-1}^n+\eta_{j-2}^n)\\
&+\tfrac{1}{2}\mu^2\frac{(\Delta t)^2}{(\Delta x)^6}(\eta_{j+3}^n-6\eta_{j+2}^n+15\eta_{j+1}^n-20\eta_j^n+15\eta_{j-1}^n-6\eta_{j-2}^n+\eta_{j-3}^n)\,.\end{aligned}\tag{5.16}$$

Clearly, the second-order accuracy is not disturbed by the addition of the small terms.

We linearize scheme (5.16) and substitute the kth term of series (4.4) after replacing s with x. After some manipulation we obtain the local amplification factor $g(k)$ as given by

$$g(k)=1-i\beta\sin\xi-\beta^2(1-\cos\xi)\,,\tag{5.17}$$

with

$$\beta=\frac{\Delta t}{\Delta x}\left[1+\varepsilon\eta-2\frac{\mu}{(\Delta x)^2}(1-\cos\xi)\right],\quad\text{and}\quad \xi=k\Delta x\,.$$

Further,

$$|g(k)|^2=1-4\beta^2(1-\beta^2)\sin^4(\tfrac{1}{2}\xi)\,.\tag{5.18}$$

For both stability and dissipation we require $|\beta|<1$, and this leads to the condition

$$\frac{\Delta t}{\Delta x}\left[1+\varepsilon|\eta|+4\frac{\mu}{(\Delta x)^2}\right]<1\,.\tag{5.19}$$

Here the damping behaves like ξ^4, provided that (5.19) is satisfied. By analogy with the derivation in the last section, we obtain for the amplitude damping and velocity ratio, respectively, the formulas

$$|T(k)|=[1-4\beta^2(1-\beta^2)\sin^4\tfrac{1}{2}\xi]^{\pi\Big/\left(\xi\frac{\Delta t}{\Delta x}\left[1+\varepsilon\eta-\frac{\mu}{(\Delta x)^2}\xi^2\right]\right)}\tag{5.20}$$

and

$$Q(k)=\arctan\left(\frac{\beta\sin\xi}{1-2\beta^2\sin^2\frac{1}{2}\xi}\right)\Big/\left(\xi\frac{\Delta t}{\Delta x}\left[1+\varepsilon\eta-\frac{\mu}{(\Delta x)^2}\xi^2\right]\right).\tag{5.21}$$

Figures 9 and 10 are graphs of $|T|$, Q, and $\arg(T)$ as given by formulas (5.20), (5.21) and (5.9).

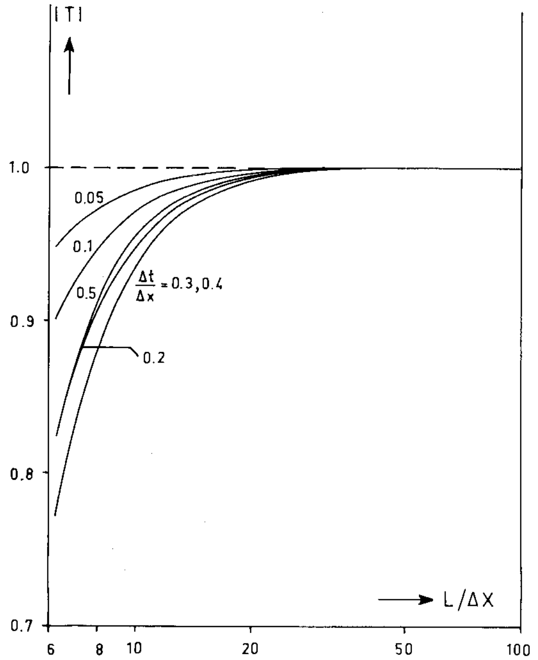

Figure 9. Scheme (5.16): Numerical damping as given by (5.20); $\varepsilon\eta = 0.7$, $\mu/(\Delta x)^2 = 0.1$.

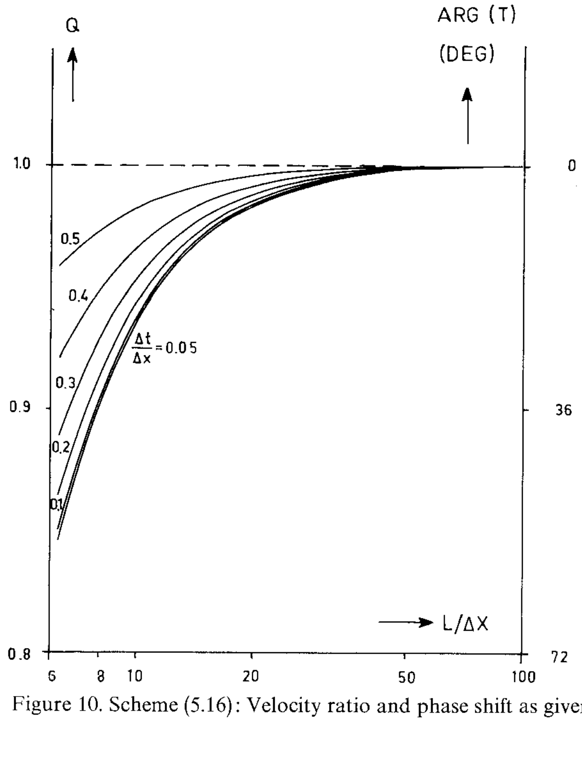

Figure 10. Scheme (5.16): Velocity ratio and phase shift as given by (5.21) and (5.9); $\varepsilon\eta = 0.7$, $\mu/(\Delta x)^2 = 0.1$.

We conclude that here the amplitude damping is much weaker than in the case of scheme (5.3). As in the case of scheme (4.1), the wave components are retarded by the discretization. If ξ is small, we have $\sin\xi \simeq \xi - \frac{1}{6}\xi^3$ and $\cos\xi \simeq 1 - \frac{1}{2}\xi^2 + \frac{1}{24}\xi^4$, and therefore,

$$g(k) = 1 - i\xi\frac{\Delta t}{\Delta x}\left[1 + \varepsilon\eta - \frac{\mu}{(\Delta x)^2}\xi^2\right] - \tfrac{1}{2}\xi^2\left(\frac{\Delta t}{\Delta x}\right)^2\left[1 + \varepsilon\eta - \frac{\mu}{(\Delta x)^2}\xi^2\right]^2 + O(\xi^3),$$

and, modulo terms $O(\xi^3)$,

$$g(k) = \exp\left\{-i\xi\frac{\Delta t}{\Delta x}\left[1+\varepsilon\eta - \frac{\mu}{(\Delta x)^2}\xi^2\right]\right\}.$$

We note that this is the exact amplification factor of equation (5.12), which is $\exp(-il\Delta t)$ with $l(k)$ as given by (5.13). Our conclusion is that the amplification factor of (5.12) also has been approximated with second-order accuracy.

In the case $\mu=0$, the scheme (5.16) is the Lax–Wendroff scheme [15] as applied to the equation $\eta_t+\eta_x+\varepsilon\eta\eta_x=0$.

5.4. *Results of Calculations*

Test calculations with the difference schemes (5.3) and (5.16), and, using the solitary wave solution (see Section 4.3) as initial function, showed that the conditions (5.5) and (5.19) can be exceeded without losing stability. In Table 1 are listed values of Δt in stable and unstable cases with some values of Δx as obtained from calculations with scheme (5.16). The corresponding quantities of excess of condition (5.19) are represented by the values of A, with

$$A = \frac{\Delta t}{\Delta x}\left[1+4\frac{\mu}{(\Delta x)^2}\right]-1\,.$$

The relatively small term $\varepsilon|\eta|$ is not considered here. The calculations were carried out for 400 time cycles, unless any instability developed earlier.

One observes that the possible excess of (5.19) without losing stability becomes smaller when the mesh is refined. It appeared that the centered scheme (4.1) does not show this feature. In our opinion, this phenomenon stems from the amplitude damping which, in turn, is caused by the truncation error (see Section 5.3).

The dissipative difference schemes (5.3) and (5.16) have been introduced among others to construct solutions of discontinuous initial-value problems. For instance, suppose that

$$\eta(x,0) = \begin{cases} 1 & \text{for } x<0 \\ 0 & \text{for } x>0\,. \end{cases} \tag{5.22}$$

is given initially.

The case $\mu=0$ leads to a homogeneous problem. It can easily be shown that the exact solution of (5.12) is then given by

$$\eta(x,t) = \begin{cases} 1 & \text{for } x/t<1+\frac{1}{2}\varepsilon \\ 0 & \text{for } x/t>1+\frac{1}{2}\varepsilon\,. \end{cases}$$

In the case $\varepsilon=0$ the exact solution of (5.12) is

$$\eta(x,t) = \int_{\zeta}^{\infty}\mathrm{Ai}(\zeta)d\zeta\,, \tag{5.23}$$

TABLE 1

Results of test calculations with scheme (5.16) *and solitary wave as initial function*; $\varepsilon=\mu=0.1$.

Δx	stable		unstable	
	Δt	A	Δt	A
0.30	0.085	0.54	0.090	0.63
0.25	0.045	0.33	0.050	0.48
0.20	0.020	0.10	0.025	0.37
0.15	0.0090	0.13	0.0095	0.19
0.10	0.0025	0.02	0.0030	0.23

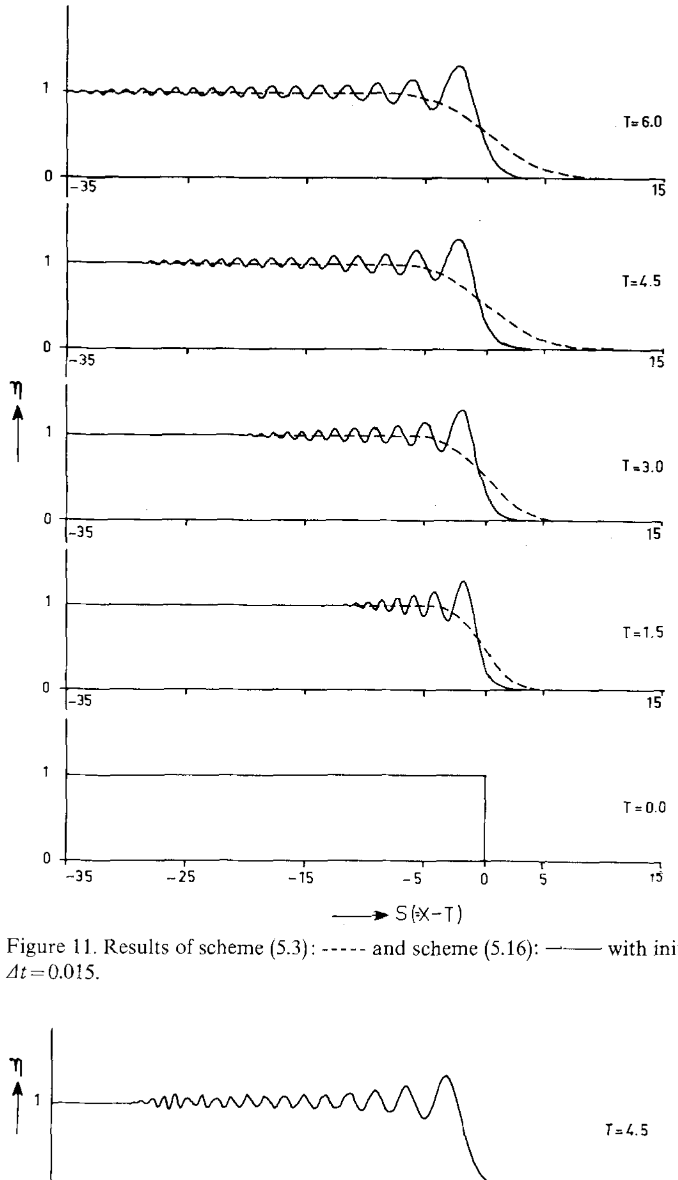

Figure 11. Results of scheme (5.3): ----- and scheme (5.16): —— with initially (5.22); $\varepsilon=0.1$, $\mu=0.1$, $\Delta x=0.2$, $\Delta t=0.015$.

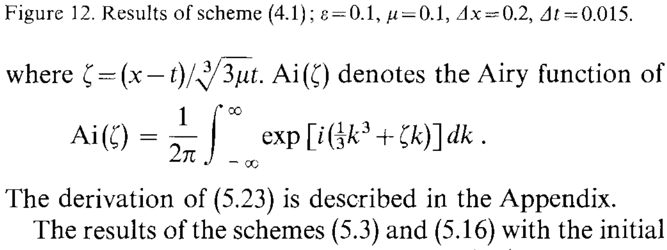

Figure 12. Results of scheme (4.1); $\varepsilon=0.1$, $\mu=0.1$, $\Delta x=0.2$, $\Delta t=0.015$.

where $\zeta=(x-t)/\sqrt[3]{3\mu t}$. $\mathrm{Ai}(\zeta)$ denotes the Airy function of the first kind, which is defined by

$$\mathrm{Ai}(\zeta) = \frac{1}{2\pi}\int_{-\infty}^{\infty} \exp\left[i\left(\tfrac{1}{3}k^3+\zeta k\right)\right] dk\,.$$

The derivation of (5.23) is described in the Appendix.

The results of the schemes (5.3) and (5.16) with the initial data (5.22) are shown in Figure 11. We conclude that the damping of scheme (5.3) which, as we have noticed in section 5.2, behaves like ξ^2, is too strong. The solitary wave pulses which are present in the solution of scheme (5.16) do not appear at all in the solution of (5.3). Instead, the initial discontinuity is transformed into a slope which continuously becomes less steep as the calculation progresses. In fact, the effect of the interaction between nonlinearity and dispersion is completely destroyed by the

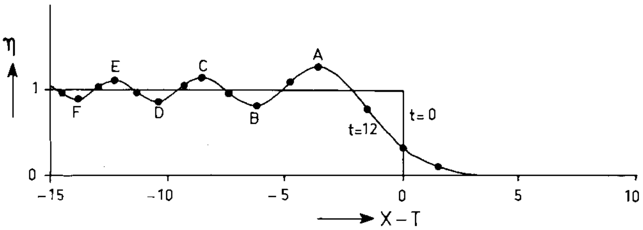

Figure 13. Exact and numerical results with initially (5.22). Dots represent results of scheme (5.16); $\Delta x = 0.2$, $\Delta t = 0.015$, $\varepsilon = 0$, $\mu = 0.1$.

TABLE 2

Exact and computed coordinates of the points A through F as shown in Figure 13.

point	exact values		computed results	
	$x-t$	η	$x-t$	η
A	−3.5	1.2738	−3.6	1.2747
B	−6.3	0.8083	−6.4	0.8077
C	−8.4	1.1549	−8.6	1.1557
D	−10.4	0.8667	−10.6	0.8668
E	−12.1	1.1179	−12.4	1.1179
F	−13.8	0.8922	−14.0	0.8914

numerical, non-physical, dissipation.

Figure 12 shows the results of the same problem as obtained using scheme (4.1). After about 700 time cycles the observed disturbances slowly moved to the left- and right-hand sides starting from the pulse on the extreme right, and leaving the solution undisturbed. However, our conclusion is that the non-dissipative scheme (4.1) is not appropriate to this problem. Additional test calculations showed that the same is true for Peregrine's scheme [16]. Though some numerical damping is present, from a linear analysis which is not given here, one can readily conclude that this scheme is not dissipative either.

The solution of equation (5.12) is shown in Figure 13 for the case $\varepsilon = 0$. The curves show the initial data at $t = 0$ as given by (5.22) and the exact solution at $t = 12$ as given by (5.23). The dots represent computed results at $t = 12$ of scheme (5.16). We conclude from (5.23) that the exact solution depends only on $(x-t)/\sqrt[3]{3\mu t}$. Thus with constant values for the mesh-sizes, advancing in time has the same effect as refining the mesh. Indeed, we observed a (rapid) convergence, and after about 200 time cycles no better agreement with the exact values was obtainable.

In Table 2 exact and numerical results have been listed for the extreme upper and lower points A through F (see Figure 13).

Notice that the linear variation of the amplitudes of the pulses as described in section 4.3 is not seen in the results which are shown in Figures 11 and 13.

Appendix

The equation

$$\eta_t + \eta_x + \mu\eta_{xxx} = 0 \tag{A.1}$$

has elementary solutions of the form

$$C_k \exp\left[i(kx - lt)\right] . \tag{A.2}$$

Here the frequency $l(k)$ is related to the wave number k by

$$l(k) = k - \mu k^3 , \tag{A.3}$$

which is obtained by substitution of (A.2) into equation (A.1).

The general solution is then given by a Fourier integral,

$$\eta(x,t) = \int_{-\infty}^{\infty} \varphi(k) \exp[i(kx-lt)]\,dk\,.$$

At the time $t=0$ we have

$$\eta(x,0) = \int_{-\infty}^{\infty} \varphi(k) \exp(ikx)\,dk\,,$$

and by virtue of (5.22) we get $\varphi(k) = -1/(2\pi ik)$, and therefore,

$$\eta(x,t) = \frac{-1}{2\pi i}\int_{-\infty}^{\infty} \frac{1}{k} \exp[i(kx-lt)]\,dk\,.$$

Substitution of (A.3) yields, after replacing μtk^3 by $\frac{1}{3}k^3$, and denoting $\zeta=(x-t)/\sqrt[3]{3\mu t}$,

$$\eta(x,t) = \frac{-1}{2\pi i}\int_{-\infty}^{\infty} \frac{1}{k} \exp[i(\tfrac{1}{3}k^3+\zeta k)]\,dk\,.$$

Hence, for $t>0$, we arrive at the solution

$$\eta(x,t) = \int_{\zeta}^{\infty} \mathrm{Ai}(\zeta)\,d\zeta\,, \tag{A.4}$$

where $\zeta=(x-t)/\sqrt[3]{3\mu t}$. $\mathrm{Ai}(\zeta)$ denotes the Airy function of the first kind, and is defined by

$$\mathrm{Ai}(\zeta) = \frac{1}{2\pi}\int_{-\infty}^{\infty} \exp[i(\tfrac{1}{3}k^3+\zeta k)]\,dk\,.$$

For details of the Airy function see, for example, [23, 24]. Indeed, T. Brooke Benjamin has remarked that (A.4) should be a solution of the KdV equation with vanishing nonlinearity (see [6]).

REFERENCES

[1] D. J. Korteweg and G. de Vries, On the change of form of long waves advancing in a rectangular canal, and on a new type of long stationary waves, *Philos. Mag.*, 39 (1895) 422–443.

[2] C. S. Gardner and G. K. Morikawa, Similarity in the asymptotic behaviour of collision-free hydromagnetic waves and water waves, New York Univ., *Courant Inst. Math. Sci.*, Res. Report NYO-9082, 1960.

[3] H. Washimi and T. Taniuti, Propagation of ion-acoustic solitary waves of small amplitude, *Phys. Rev. Letters*, 17 (1966) 996–998.

[4] M. D. Kruskal, Asymptotology in numerical computation: progress and plans on the Fermi-Pasta-Ulam problem, *Proceedings of the IBM Scientific Computing Symposium on Large-Scale Problems in Physics* (1965).

[5] N. J. Zabusky, A synergetic approach to problems of nonlinear dispersive wave propagation and interaction, *Nonlinear Partial Differential Equations*, Academic Press, New York (1967).

[6] L. van Wijngaarden, Linear and non-linear dispersion of pressure pulses in liquid-bubble mixtures, *6th Symposium on Naval Hydrodynamics*, Washington D.C. (1966).

[7] L. van Wijngaarden, On the equations of motion for mixtures of liquid and gas bubbles, *J. Fluid Mech.*, 33 (1968) 465–474.

[8] A. Sjöberg, *On the Korteweg–de Vries equation*, Uppsala Univ., Dept. of Computer Sci., Report, 1967.

[9] P. D. Lax, Integrals of nonlinear equations of evolution and solitary waves, *Comm. Pure Appl. Math.*, 21 (1968) 467–490.

[10] L. J. F. Broer, On the interaction of non-linearity and dispersion in wave propagation: II. Approximate solutions of the reduced Boussinesq equation, *Appl. sci. Res.*, Section B, 12 (1965) 113–129.

[11] H. W. Hoogstraten, *On non-linear dispersive water waves*, Doctoral Thesis, Delft University of Technology (1968).

[12] C. S. Gardner, J. M. Greene, M. D. Kruskal and R. M. Miura, Method for solving the Korteweg–de Vries equation, *Phys. Rev. Letters*, 19 (1967) 1095–1097.

[13] N. J. Zabusky and M. D. Kruskal, Interaction of "solitons" in a collisionless plasma and the recurrence of initial states, *Phys. Rev. Letters*, 15 (1965) 240–243.

[14] P. D. Lax, Weak solutions of nonlinear hyperbolic equations and their numerical computation, *Comm. Pure Appl. Math.*, 7 (1954) 159–193.

[15] P. D. Lax and B. Wendroff, Systems of conservation laws, *Comm. Pure Appl. Math.*, 13 (1960) 217–237.

[16] D. H. Peregrine, Calculations of the development of an undular bore, *J. Fluid Mech.*, 25, 2 (1966) 321–330.
[17] N. A. Phillips, Numerical weather prediction, *Advances in Computers*, Vol. 1, Academic Press, New York (1960).
[18] A. C. Vliegenthart, Dissipative difference schemes for shallow water equations, *J. Eng. Maths.*, 3 (1969) 81–94.
[19] K. V. Roberts and N. O. Weiss, Convective difference schemes, *Math. Computation*, 20 (1966) 94.
[20] R. D. Richtmyer and K. W. Morton, *Difference methods for initial-value problems*, Second Edition, Interscience Publishers, New York (1967).
[21] J. J. Leendertse, *Aspects of a computational model for long-period water-wave propagation*, Doctoral Thesis, Delft University of Technology (1967).
[22] L. J. F. Broer, On the interaction of non-linearity and dispersion in wave propagation: I. Boussinesq's equation, *Appl. sci. Res.*, Section B, 11 (1965) 273–285.
[23] J. C. P. Miller, *The Airy integral*, British Assoc. Adv. Sci. Math. Tables, Part-vol. B, Cambridge Univ. Press, Cambridge (1946).
[24] M. Abramowitz and I. A. Stegun, *Handbook of mathematical functions*, Dover Publications, Inc., New York.

Journal of Engineering Math., Vol. 5 (1971) 137–155